

The structure and conductivity of $\text{LaMn}_{1-z}\text{Cr}_z\text{O}_3$ and $(\text{La}, \text{A})_{1-y}\text{Mn}_{1-z}\text{Cr}_z\text{O}_3$ ($\text{A} = \text{Sr}, \text{Ca}$) as air cathodes in solid oxide fuel cells

M. B. PHILLIPPS, N. M. SAMMES*

Centre for Technology, The University of Waikato, Private Bag 3105, Hamilton, New Zealand

O. YAMAMOTO

Dept. of Chemistry, Mie University, Kamihama-cho, Tsu, 514, Japan

Doped LaMnO_3 systems are used as cathodes in solid oxide fuel cells, mainly due to their high electronic conductivity, thermal matching to the electrolyte material and good catalytic activity towards oxygen reduction. Lanthanum deficient LaMnO_3 has been shown to have a higher electronic conductivity than stoichiometric LaMnO_3 , however, the material has been found to sinter more readily causing a reduction in the efficiency of the cathode. This paper discusses the effect of imparting non-stoichiometry to the LaMnO_3 system with the incorporation of a B site dopant, Cr. The paper examines the effect on the conductivity and phase present with increased Cr content, and shows that Cr in $\text{LaMn}_{1-z}\text{Cr}_z\text{O}_3$, up to $z = 0.15$, does not produce an unacceptably large decrease in the electronic conductivity, especially for a Ca doped, A site deficient system. Thus, a B site doped system is considered as a possible candidate for solid oxide fuel cell cathode systems.

1. Introduction

For solid oxide fuel cell (SOFC) applications, doped lanthanum manganite (LaMnO_3) is the popular choice for the cathode, meeting most of the requirements of similar thermal expansivity, high electronic conductivity, good catalytic activity towards oxygen reduction, chemical stability, etc. LaMnO_3 has the perovskite structure (ABO_3) and at high temperature exhibits oxygen non-stoichiometry ($\text{LaMnO}_{3-\delta}$) [1, 2]. It is a p-type semiconductor, inherently due to the cation vacancies formed by the lanthanum non-stoichiometry. Hence, conductivity of this species may be enhanced by substituting lower valent cations onto either A or B sites; Sr, Ca, Ba, Ni, Cr, Na, Co, Mg for example, have been studied [3, 4]. Of these, strontium and calcium are favoured as A site dopants because of the high electronic conductivity that is found in the doped LaMnO_3 in an oxidizing environment. For example, Sr^{2+} replaces La^{3+} , increasing the Mn^{4+} content and thus the charge carrier concentration.

Properties of the perovskite-type oxides are primarily determined by the B site ion, because the highly electronic conducting oxides exhibit mixed valencies on the B site. A site composition also affects the electronic conductivity of the oxides via charge compensation and by increasing the extent of mixed-valent states. Transition metals, on the B site of a perovskite type oxide, are useful from an electrical perspective.

LaMnO_3 and LaCrO_3 (where La is 3+) have their B sites occupied by metals in both the 3+ and 4+ valence states.

In this work, the structure and electrical conductivity of the non-stoichiometric LaMnO_3 system is examined, with the effect of B site substitution (using Cr). By using Cr as a B site substituent, the sinterability of the highly sinterable lanthanum deficient manganite should be retarded, thus allowing for a stable electrode with good morphological properties. The electrical conductivity of this system may be compromised, somewhat, however the reactivity with yttria stabilized zirconia (YSZ), at 1273 K, is expected to be low [3]. It has also been shown that degradation of the electrode during high fabrication temperatures, and subsequent increase of overvoltage, can be minimized with Cr doping [5], although it would be larger than the non B site doped system [6]. Primarily, this work investigated the phases and electrical conductivity of the mixed B site composition with further study focusing on A site doped, A site deficient, compositions of this system.

2. Experimental procedure

$\text{LaMn}_{1-z}\text{Cr}_z\text{O}_3$ (LMCr, $z = 0-0.5$) and $(\text{La}_{1-x}\text{A}_x)_{1-y}\text{Mn}_{1-z}\text{Cr}_z\text{O}_3$ (LSMCr for $\text{A} = \text{Sr}$, $x = 0.2$; LCMCr for $\text{A} = \text{Ca}$, $x = 0.5$) powders for $y = 0.1$ and

*Author to whom correspondence should be addressed.

$z = 0-0.2$ were synthesized via a self propagating combustion method, using glycine as a fuel, as described by Chick *et al.* [7]. Stoichiometric amounts of the metal nitrates (99% purity) were dissolved in a minimum of distilled water, comprising the oxidizer. Glycine (amino-acetic acid) was used as the fuel, in amounts to remove excess nitrate via stoichiometric combustion and producing the desired oxide. The resulting fine, light, voluminous powders were then fired at 1173–1273 K for 12–20 h to ensure complete oxidation of the organics and the complete production of the perovskite phase.

LMCr powders were uniaxially pressed into round pellets for rapid quenching in liquid nitrogen from various soak temperatures, and subsequent analysis of X-ray diffraction (XRD) characteristics, using Cu K α radiation with a conventional Bragg–Brentano goniometer (Philips PW1050). Room temperature XRD was performed on the LSMCr and LMCr powered samples using a Rigaku RC (12 kW) with monochromated Cu K α radiation.

Rectangular bars were uniaxially pressed for measuring the high temperature electrical conductivity using the standard DC four terminal method. The LMCr series were fired at 1573 K for 1 h, and the relative density was measured using the standard Archimedes' method, and thus the conductivity data collected was normalized for density differences [8]. The LSMCr and LMCr sample bars were fired at 1673 K, yielding densities > 90% of theoretical.

3. Results and discussion

Crystal structures observed from XRD of the LMCr series, quenched from temperatures ranging from 873–1673 K, are shown in Fig. 1. The XRD patterns were assigned to three main types; rhombohedral–hexagonal, orthorhombic and an orthorhombic intermediate of these two types (denoted 'intermediate'), from comparisons with the literature [9]. As the chromium content increases, the orthorhombic intermediate phase is seen to shift to lower sintering temperatures. The classical orthorhombic structure was observed for the $y = 0.3$ sample at 1573 K and above.

In accordance with Takeda *et al.* [9], it can be postulated that the lanthanum deficient samples examined in this work had a high oxygen excess, due

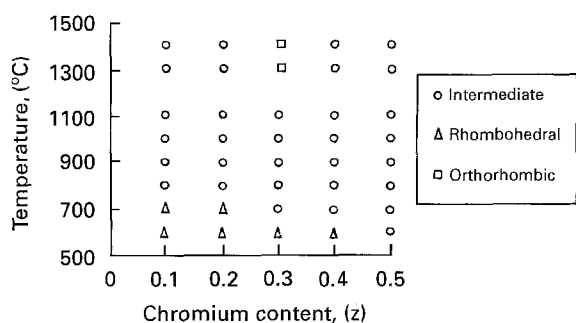


Figure 1 Phases observed at various temperatures for the LMCr system.

to the rhombohedral phase being observed. A decrease in cell volume, with increase in oxygen, is evidence of cation defects rather than interstitial oxygen because of the smaller radius of Mn⁴⁺ [10]. Low Mn⁴⁺ content is characterized by an orthorhombic symmetry, with high distortion from the ideal perovskite. This is caused by ordering of Jahn–Teller distorted Mn³⁺O₆ octahedra. The t_{2g}³e_g state for octahedral Mn(III), because of the odd number of e_g electrons (d⁴), is subject to Jahn–Teller distortion, and this is often observed as a considerable elongation of the two trans bonds. The ordering is then broken when the Mn⁴⁺ concentration increases, resulting in different orthorhombic patterns and rhombohedral–hexagonal symmetry at high Mn⁴⁺ content, with only the low spin d³ state. These outlined structures, are seen when the La:Mn ratio is equal to one, but when the ratio deviates, different patterns are observed. A comprehensive account of these is given by van Roosmalen *et al.* [11]. The phase transition from orthorhombic to rhombohedral–hexagonal shifts to a lower temperature for higher values of δ , due to the effective change in Mn⁴⁺ content with different annealing regimes.

When B site substitution occurs, the change in the A–O/B–O averaged bond distance ratio, affects the observed phases [10]. As the ratio increases for the LaMnO₃ and LaCrO₃ systems, the rhombohedral–hexagonal phase is favoured. Hence, when small ions, such as Mn⁴⁺ and/or Cr⁴⁺, are introduced to the B site, the orthorhombic to rhombohedral–hexagonal phase transition is lowered, as is seen in Fig. 1. The p-type conductivity in these systems is characterized by an overall increase in the Mn⁴⁺ ions and therefore the charge carrier concentration [12].

Conductivity of the LMCr series (from $z = 0-0.5$) is shown in Fig. 2. With increasing z , the electronic conductivity was found to decrease, due to a decrease in the Mn concentration on the B sites which are thought to dominate the conduction process.

After assessing the effect of Cr addition, it followed to examine the effect of A site substitution in an A site deficient system, with Cr content $z = 0-0.15$. By decreasing the La:Mn ratio, and introducing Sr²⁺ ions onto the A site, an increase in Mn⁴⁺ concentration was expected, and hence an increase in electronic conductivity [12]. B site substitution in the LSMCr series showed a distinct structural change from the orthorhombic structure (at $z = 0$) to the hexagonal (at $z > 0$), based on LaAlO₃ (R3c), with decreased distortion as described by Takeda *et al.* [9]. There was

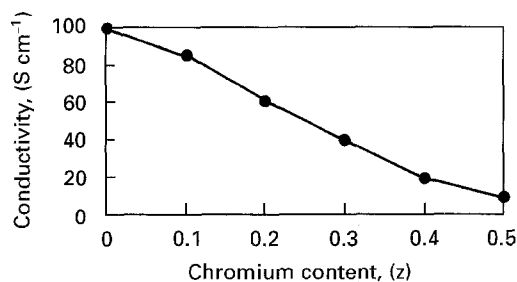


Figure 2 Electrical conductivity of the LMCr system at 1273 K.

TABLE I Lattice parameters for the $(\text{La}_{0.8}\text{Sr}_{0.2})_{0.9}\text{Mn}_{1-z}\text{Cr}_z\text{O}_3$ system. Numbers in parentheses indicate standard deviations.

z	$a \times 10^{-1}$ (nm)	$b \times 10^{-1}$ (nm)	$c \times 10^{-1}$ (nm)	Structure	Cell volume nm^3
0.0	5.455(6)	5.508(2)	7.730(7)	Orthorhombic	232.7(4)
0.05	5.511(3)	–	13.38(1)	Hexagonal	352.0(5)
0.1	5.506(2)	–	13.351(8)	Hexagonal	350.6(3)
0.15	5.508(2)	–	13.357(8)	Hexagonal	350.9(3)

TABLE II Lattice parameters for the $(\text{La}_{0.5}\text{Ca}_{0.5})_{0.9}\text{Mn}_{1-z}\text{Cr}_z\text{O}_3$ system. Numbers in parentheses indicate standard deviations

z	$a \times 10^{-1}$ (nm)	$b \times 10^{-1}$ (nm)	$c \times 10^{-1}$ (nm)	Structure	Cell volume nm^3
0.0	5.421(3)	5.410(2)	7.656(5)	Orthorhombic	224.5(2)
0.05	5.377(6)	5.407(5)	7.65(1)	Orthorhombic	222.4(5)
0.1	5.416(3)	5.405(2)	7.645(6)	Orthorhombic	223.8(2)
0.15	5.4202(5)	5.4145(4)	7.646(1)	Orthorhombic	224.41(4)

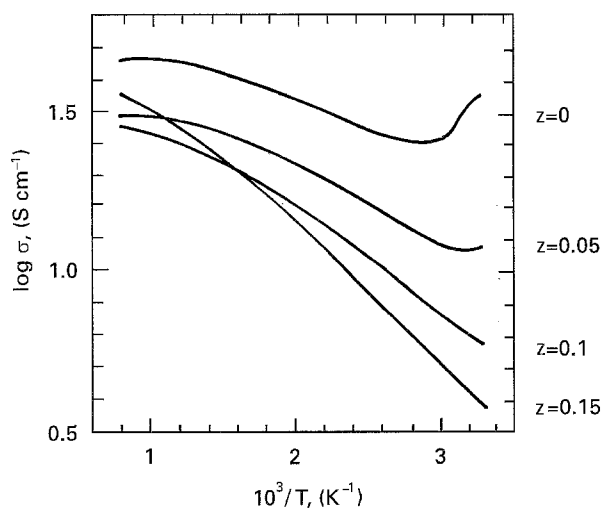


Figure 3 Temperature dependence of electrical conductivity for $(\text{La}_{0.8}\text{Sr}_{0.2})_{0.9}\text{Mn}_{1-z}\text{Cr}_z\text{O}_3$.

also a general decrease in the observed cell volume, with increasing Cr content, as shown in Table I. This can be explained by an ionic size effect of the smaller Cr^{3+} ion. Lattice parameters, calculated using a least squares analysis program, are presented in Table I.

The LCMCr systems all displayed orthorhombic structures similar to the $(\text{La}_{0.8}\text{Sr}_{0.2})_{0.9}\text{MnO}_3$ composition. A small amount of the secondary phase, CaMnO_3 , was observed in the compositions $z = 0, 0.05$ and 0.1 , with a slight increase in intensity with increasing z . Lattice parameters are shown in Table II. The cell volume initially decreased with addition of Cr, as expected with ionic size effects, however, a slight increase was then observed as the Cr content increased. This could be explained by the subsequent effect of reduction in the Mn^{4+} content and hence an increase in the Jahn–Teller distortion as described above. It can be postulated that this effect was observed for the Ca doped species, rather than the Sr doped, due to a greater Mn^{4+} concentration imparted to the LCMCr system via heavier A site doping, which can be supported by observations of electrical conductivity.

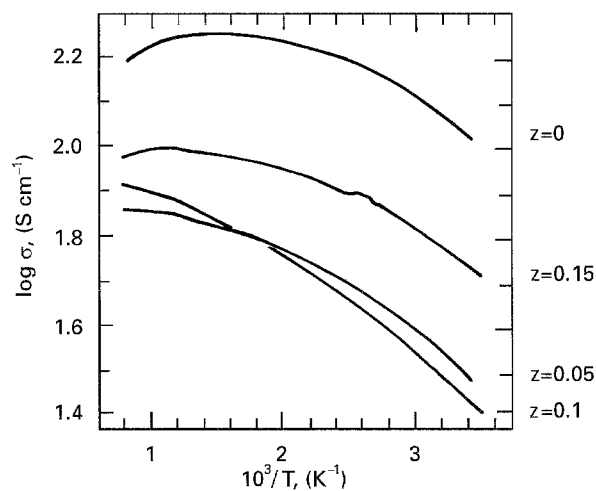


Figure 4 Temperature dependence of electrical conductivity for $(\text{La}_{0.5}\text{Ca}_{0.5})_{0.9}\text{Mn}_{1-z}\text{Cr}_z\text{O}_3$.

Fig. 3 shows the temperature dependence of the electrical conductivity of LSMCr. The conductivity of this system was semiconductive throughout the composition range, and was rather low, being in the region of $27\text{--}52 \text{ S cm}^{-1}$ at 1273 K . A decrease was observed with increasing Cr content, however the $z = 0.15$ species showed almost the same behaviour as the $z = 0.05$ composition at 1273 K , as can be seen in Fig. 3.

The LCMCr system displayed much better behaviour than the Sr doped compositions, with values above 70 S cm^{-1} at 1273 K as observed in Fig. 4. The $z = 0.05$ and 0.01 samples showed much lower conductivity values than the $z = 0.15$ sample. This is probably due to the small amount of CaMnO_3 phase detected in these samples, although an empirical expectation of gradual decrease in conductivity with Cr addition is not always necessary, as seen in the results of Mori *et al.* [5]. Obviously the non B site doped specimen was not drastically affected by the presence of this second phase, with a conductivity value of approximately 160 S cm^{-1} at 1273 K . This sample did, however, show a change to metallic conduction above 1273 K , with the $z = 0.15$ sample showing

similar behaviour. Further work is currently being undertaken to investigate the long term stability of these materials for application as cathodes.

4. Conclusions

It was observed that by adding Cr, as a B site dopant at low levels (< 20 mol %) in an A site deficient, A site doped lanthanum manganite system, the electrical conductivity was not particularly adversely affected. Because advantages do arise from such a system, over the undoped material, this configuration should be considered as one for application as an air electrode in a SOFC.

References

1. J. A. M. VAN ROOSMALEN and E. H. P. CORDFUNKE, *J. Solid State Chem.* **93** (1991) 212.
2. S. OTOSHI, H. SASAKI, H. OHNISHI, M. HASE, K. ISHIMARU, M. IPPOMMATSU, T. HIGUCHI, M. MIYAYAMA and H. YANAGIDA, *J. Electrochem. Soc.* **138** (1991) 1519.
3. H. YOKOKAWA, N. SAKAI, T. KAWADA and M. DOKIYA, *Denki Kagaku* **57** (1989) 821.
4. R. HILDRUM, S. AASLAND and Ø. JOHANNESSEN, *Solid State Ionics* **66** (1993) 207.
5. M. MORI, N. SAKAI, T. KAWADA, H. YOKOKAWA and M. DOKIYA, *Denki Kagaku* **58** (1990) 528.
6. Y. TAKEDA, O. YAMAMOTO, M. NODA and R. KANNO, *J. Electrochem. Soc.* **134** (1987) 2565.
7. L. A. CHICK, J. L. BATES, L. R. PEDERSON and H. E. KISSINGER, in "Proceedings of the First International Symposium on Solid Oxide Fuel Cells", Pennington N.J., 1989, edited by S.C. Singhal (The Electrochemical Society, Pennington N.J. 1989) p. 170.
8. F. S. BRUGNER and R. N. BLUMENTHAL, *J. Am. Ceram. Soc.* **54** (1971) 57.
9. Y. TAKEDA, S. NAKAI, T. KOJIMA, R. KANNO, N. IMANISHI, G. Q. SHEN and O. YAMAMOTO, *Mat. Res. Bull.* **26** (1991) 153.
10. S. A. HOWARD, J. YAU and H. U. ANDERSON, *J. Am. Ceram. Soc.* **75** (1991) 1685.
11. J. A. M. VAN ROOSMALEN, P. VAN VLAANDEREN, E. H. P. CORDFUNKE, W. L. IJDO and D. J. W. IJDO, submitted to *J. Solid State Chem.*
12. J. A. M. VAN ROOSMALEN, J. P. P. HUIJSMANS and L. PLOMP, *Solid State Ionics* **66** (1993) 279.

Received 7 June 1995

and accepted 20 November 1995